The critical temperature of a superconductor on a possible $E \cdot p$ mediated pairing mechanism

2006 J. Phys.: Condens. Matter 18 143

(http://iopscience.iop.org/0953-8984/18/1/011)

INSTITUTE OF PHYSICS PUBLISHING JOURNAL OF PHYSICS: CONDENSED MATTER

J. Phys.: Condens. Matter **18** (2006) 143–164 doi:10.1088/0953-8984/18/1/011

The critical temperature of a superconductor on a possible $E \cdot p$ mediated pairing mechanism

C M Srivastava

Department of Physics, Indian Institute of Technology, Powai, Mumbai-400 076, India

Received 28 June 2005, in final form 30 September 2005
Published 9 December 2005
Online at stacks.iop.org/JPhysCM/18/143

Abstract

The possibility of pairing correlations arising from the quenching of the repulsive electron–ion Darwin term in the pairon (Cooper pair) state is examined. Two pairing processes, arising from ionic density fluctuations (phonons) and from electronic density fluctuations (excitons), are shown to dominate in low T_c and high T_c superconductors, respectively. Based on a two-body $\boldsymbol{E} \cdot \boldsymbol{p}$ interaction potential the BCS type of wavefunction and reduced Hamiltonian are obtained. As quenching occurs only when a pairon is scattered by the nucleus without recoil between an electron and a hole section of the Fermi surface, a two-band model with umklapp processes gives the T_c equation for both the phonon- and exciton-coupled superconductors whose solution is similar to that obtained by Eliashberg equations except that the dependence of T_c on structure is explicitly included.

1. Introduction

The BCS theory in the Eliashberg form with a retarded electron–phonon interaction and Coulomb repulsion remains today a remarkably complete theory of the superconducting state [1]. The main support for the model is obtained from the isotope effect and near equality of the phonon spectral functions $\alpha^2 F(\omega)$ obtained from tunnelling experiments and $g(\omega)$, the phonon density of states, from neutron scattering. Despite its immense success, the BCS theory and its refinements like the Eliashberg theory have not led to the prediction of T_c [2]. The discovery of high T_c layered oxide superconductor with T_c more than 125 K and almost vanishing isotope effect has led to some suggestions that in oxides magnetic excitations could lead to the two-body attractive interaction with higher coupling strength compared to phonon coupling [3, 4]. But this is not supported by the discovery of superconductivity in MgB_2 with no copper atoms and T_c higher than in metals and alloys [5].

The present strong-coupling theory of superconductivity assumes that the total interaction comprising a phonon-induced attractive interaction and the Coulomb interaction produces an effective two-body coupling, expressed by $(\lambda - \mu^*)$, which leads to superconductivity if λ exceeds μ^*. In the $\boldsymbol{E} \cdot \boldsymbol{p}$ model, there is an additional phonon-induced coupling, λ^D, for

s electrons only. This arises from the Darwin term interaction that exists between the electron and the ion and the electron and other electrons, the former being strong and repulsive and the latter weak and attractive. It is shown that this repulsive interaction is quenched when a pair of electrons is scattered, to and fro, without recoil by the nucleus from an electron to a hole section at the Fermi surface and thereby provides for the condensation energy. If the scattering is with the recoil of the nucleus the $\boldsymbol{E} \cdot \boldsymbol{p}$ repulsive energy remains unchanged from that in the normal state. This approach gives the experimentally adjusted T_c equation obtained by McMillan using Eliashberg equations [6].

The motion of the Cooper pair in the lattice is described in terms of two variables which are separable, one relating to internal coordinates and the other to the centroid's coordinates. The Schrödinger equation for the internal coordinates is found to be of a particle of reduced mass, $\mu = m/2$, charge $e^* = 2e$ and spin zero, where m and e are the mass and charge of the electron, while that for the external coordinates is the Schrödinger equation for a free particle of mass $m^* = 2m$. The total energy including the $\boldsymbol{E} \cdot \boldsymbol{p}$ energy breaks up into the sum of internal energy and the energy of translation. This wavefunction accounts for the finite momentum density of the superfluid along with its quantum phase and depends on both the internal and external coordinates of the particle, called here a pairon.

The pairon–nucleus $\boldsymbol{E} \cdot \boldsymbol{p}$ scattering is described as a s-wave scattering of a particle of mass m^* by a deep and narrow potential well of scattering length $e^{*2}/\mu c^2$. The potential is a two-body delta-function potential similar to that used in neutron scattering and thereby explains many of the puzzling results of tunnelling in superconductors. Further, this approach addresses some of the aspects of superconductivity that are beyond the grasp of the present Migdal–Eliashberg theory, like the dependence of superconductivity on crystal structure [2].

We have empirically shown that the repulsive electron–ion $\boldsymbol{E} \cdot \boldsymbol{p}$ interaction energy vanishes in the time-reversed pair state if it continuously scatters from a hole to an electron pocket at the Fermi surface and thereby accounts for Cooper condensation [7]. We present here a detailed study of this model and show that the BCS reduced Hamiltonian and wavefunction follow naturally from this model on appropriately defining the two-body interaction potential produced by ionic density fluctuations (phonons) in low temperature superconductors and electronic density fluctuations (excitons) in high T_c superconductors. Recently it has been proposed that Darwin interaction plays a role in superconductivity but the treatment is confined to semi-classical electrons and does not extend to the calculation of the critical temperature [8, 9].

In section 2 estimates of Darwin term energy in atoms are discussed and in section 3 the electron–ion Hamiltonian including the $\boldsymbol{E} \cdot \boldsymbol{p}$ interaction is presented. The BCS-like wavefunction and reduced Hamiltonian using the two-body $\boldsymbol{E} \cdot \boldsymbol{p}$ interaction potential is obtained in section 4 and solutions for T_c are discussed in section 5. The superconductivity in oxides based on the exciton mechanism is discussed in section 6.

2. Estimate of the Darwin term

The semi-metallic properties of $BaPbO_3$ have been examined by Matheiss and Hamann [10], who have concluded that 6s–2p overlap in this system is a consequence of the Darwin and mass–velocity correction terms. Their conclusion is based on the estimates of these energies by Baschelet and Schuter using relativistic conserving pseudopotentials [11]. They have shown that the ns binding energy of group IV elements C, Si, Ge, Sn and Pb increased as a consequence of the combined effect of these two terms to 16.3, 48.9, 337, 745 and 2500 meV respectively. Using a non-relativistic hydrogen wavefunction the energies of the two terms can be decoupled. We obtain the energy for the Darwin term (atomic) as 26.1, 42.3, 65.2, 91.7 and 3050 meV,

respectively, for these elements. As the pairing correlation energy per electron is less than 3.5 meV for low T_c and less than 25 meV for high T_c superconductors, the Darwin term interaction has the necessary strength to produce the Cooper pairing state.

In section 4 it is shown that electron–ion and electron–electron $\boldsymbol{E}\cdot\boldsymbol{p}$ interaction energies vanish for the time-reversed pairs near the Fermi surface and the state of the quenched $\boldsymbol{E}\cdot\boldsymbol{p}$ energy is described by the BCS reduced Hamiltonian and wavefunction. In the present model pairons (Cooper pairs) are formed due to recoilless scattering by the nucleus from an electron to a hole section at the Fermi surface that quenches the $\boldsymbol{E}\cdot\boldsymbol{p}$ energy. Solutions for T_c on this model and those obtained from Eliashberg equations are discussed in section 5 for low T_c and in section 6 for high T_c superconductors.

3. Electron–ion Hamiltonian including the Darwin term

The Hamiltonian for the system of electrons including the $\boldsymbol{E}\cdot\boldsymbol{p}$ interaction in the adiabatic approximation can be written as

$$H_e = \sum_i \frac{p_i^2}{2m} + \sum_{i,\nu} V(x_i - X_\nu) + 1/2 \sum_{i\neq j} \frac{e^2}{|x_i - x_j|} + \frac{\pi}{2}\left(\frac{e^2\hbar^2}{m^2c^2}\right)\left[\sum_{i,\nu} z\delta(x_i - X_\nu) - \sum_{i>j}\delta(x_i - x_j)\right]. \tag{1}$$

We take one ion per unit cell and assume X_ν as the position of the νth ion and x_i as the position of the ith conduction electron. Successive terms on the right in equation (1) are the kinetic energy of the electron, the ei interaction, the ee interaction and the ei and the ee Darwin term. Here we have assumed that ei and ee Darwin terms can be written as delta-function potentials, with z as the valence ion charge.

The Hamiltonian including the $\boldsymbol{E}\cdot\boldsymbol{p}$ term using electron and phonon operators and Nambu's technique can be written as [12]

$$\psi_k = \begin{vmatrix} c_{k\uparrow} \\ c^+_{-k\downarrow} \end{vmatrix} \qquad \psi^+_k = \left|c^+_{k\uparrow}, c_{-k\downarrow}\right|$$

$$\tau_1 = \begin{vmatrix} 0 & 1 \\ 1 & 0 \end{vmatrix}, \qquad \tau_2 = \begin{vmatrix} 0 & -\mathrm{i} \\ \mathrm{i} & 0 \end{vmatrix}, \qquad \tau_3 = \begin{vmatrix} 1 & 0 \\ 0 & -1 \end{vmatrix}, \qquad \tau_4 = \begin{vmatrix} 1 & 0 \\ 0 & 1 \end{vmatrix}$$

$$H = \sum_k E_k \psi^+_k \tau_3 \psi_k + \sum_{q,\lambda} \Omega_{q\lambda}(b^+_{q\lambda} b_{q\lambda} + 1/2) + \sum_{q,k}(V(q) + \beta)S(q)\psi^+_{k+q}\tau_3\psi_k + \tfrac{1}{2}\sum_{k,q}\left(\frac{4\pi e^2}{q^2} + \beta'\right)(\psi^+_{k-q}\tau_3\psi_k)(\psi^+_{k'+q}\tau_3\psi_{k'}) + \left(\sum_{k,q,\lambda} g^{\mathrm{F}}_{kq\lambda}\psi^+_{k+q}\tau_3\psi_k + \sum g^{\mathrm{D}}_{kKq\lambda}S(q)\psi^+_{k+K+q}\tau_3\psi_k\right)\phi_{q,\lambda}. \tag{2}$$

Here ψ_k is a two-component electron field operator for a time reversed pair $(k\uparrow, -k\downarrow)$ and ψ^+_k is its adjoint, $c_{k\uparrow}$ ($c^+_{k\uparrow}$) destroys (creates) an electron of momentum k and spin up, $b_{q\lambda}$ ($b^+_{q\lambda}$) destroys (creates) a phonon of wavevector q and polarization λ, $\phi_{q\lambda}$ is the phonon field operator and τ_i are Pauli spin matrices. The first two terms in equation (2) describe the bare electron and bare phonon energies, respectively. The third term is the electron–rigid lattice interaction with $V(q)$ and β representing the Fourier transform of the electron–ion and Darwin term pseudo-potentials, respectively, and $S(q)$ is the structure factor. The fourth term is the

Coulomb and Darwin term interactions between the electrons. The final term is the electron–phonon interaction arising from the Fröhlich Hamiltonian and Darwin term pseudo-potential, respectively,

$$g^{\mathrm{F}}_{kq\lambda} = \left(\frac{\hbar}{2M\Omega_{q\lambda}}\right)^{1/2} \sum_{\nu} \langle k+q|\nabla_\nu V|k\rangle \epsilon_{q\lambda\nu} \tag{3}$$

$$g^{\mathrm{D}}_{kKq\lambda} = \left(\frac{\hbar}{2M\Omega_{q\lambda}}\right)^{1/2} \sum_{\nu} \langle k+K+q\,|\beta_\nu|\,k\rangle \epsilon_{qK\lambda\nu}(K+q) \tag{4}$$

where $\epsilon_{q\lambda\nu}(\epsilon_{qk\lambda\nu}) = \delta X^{q\lambda}_\nu/|\delta X^{q\lambda}_\nu|(\delta X^{qK\lambda}_\nu/|\delta X^{qK\lambda}_\nu|)$ and $\delta X^{q\lambda}_\nu(\delta X^{qK\lambda}_\nu)$ is the ion displacement at lattice site ν that produces the phonon frequency, $\Omega_{q\lambda}$, wavevector $q\,(q+K)$ and polarization λ.

Further

$$S(q) = \sum_{\nu} \exp(\mathrm{i}q\cdot X_\nu) \tag{5}$$

$$\beta = \frac{\pi}{2}\frac{e^2\hbar^2}{m^2c^2} z\langle\delta(x)\rangle, \qquad \beta' = -\frac{\pi}{2}\frac{e^2\hbar^2}{m^2c^2}\langle\delta(x_{12})\rangle \tag{6}$$

$$\Phi_{q\lambda} = (b_{q\lambda} + b^{+}_{-q\lambda}). \tag{7}$$

The Hamiltonian in equation (2) is now used to construct the electronic self-energy Σ which is defined by the Dyson's equation.

$$G^{-1}(k, \mathrm{i}\omega_n) = G_0^{-1}(k, \mathrm{i}\omega_n) - \sum(k, i\omega_n).$$

The self-energy will have contributions from electron–static lattice, electron–phonon and electron–electron interactions that appear in third, fourth and fifth terms in equation (2). Since each of the contributions has two components of which one is from the Darwin term,

$$\sum = \sum^{F}_{\mathrm{ep}} + \sum^{D}_{\mathrm{ep}} + \sum^{O}_{\mathrm{el}} + \sum^{D}_{\mathrm{el}} + \sum^{O}_{\mathrm{ee}} + \sum^{D}_{\mathrm{ee}} \tag{8}$$

where the superscript F denotes the electron–phonon self-energy for the Fröhlich-type pseudopotential, D the Darwin term and O the electrostatic energy of interacting ions and electrons in a uniform compensating charge distribution denoted by the first component in the third and fourth terms in equation (2).

The self-energy in the superconducting state is written in terms of four parameters Z, χ, ϕ and $\bar{\phi}$ [1]

$$\sum(k, \mathrm{i}\omega_n) = \mathrm{i}\omega_n[1 - Z(k, \mathrm{i}\omega_n)]\tau_4 + \chi(k, \mathrm{i}\omega_n)\tau_3 + \phi(k, \mathrm{i}\omega_n)\tau_1 + \bar{\phi}(k, \mathrm{i}\omega_n)\tau_2. \tag{9}$$

Here the function $\phi(k, \mathrm{i}\omega_\mathrm{n})$ is the order parameter and $Z\ (k, \mathrm{i}\omega_\mathrm{n})$ and $\chi\ (k, \mathrm{i}\omega_\mathrm{n})$ represent the renormalization of the electron spectrum and change little when the material goes from superconducting to normal phase. It is found that χ vanishes when the Green's function in the intermediate state is averaged over the states at the Fermi surface [2]. Further for homogeneous superconductors in the absence of a magnetic field it is possible to choose a gauge in which $\bar{\phi} = 0$. We are then left with only two unknown functions, Z and ϕ, which are solved self-consistently using Eliashberg equations to obtain the critical temperature T_c. This solution for T_c is shown in section 5 to arise from the recoilless collision of the pairon with the nucleus for the zero energy transfer using Lipkin's sum rule [13].

The pair function ϕ determines the gap function $\Delta(\omega)$ in the energy spectrum for $T < T_\mathrm{c}$ and can be written as

$$\phi(\omega) = \sum_i Z(\omega)\Delta_i(\omega) \qquad (i = \mathrm{ep}, \mathrm{el}, \mathrm{ee}). \tag{10}$$

It is shown in section 5 that the phonon induced pair field in which $\boldsymbol{E}\cdot\boldsymbol{p}$ energy vanishes arises due to transitions of the pairon between the electron and hole sections of the Fermi surface through emission or absorption of phonons by the nucleus without any energy transfer to or from the lattice vibrations, as in the Mossbauer effect. The el contribution originates from the third term in equation (2) and describes the effect of electronic density fluctuations that screen the ionic pseudopotential. These interactions appear in the cohesive energy of solids and are described as the effect of bandgap on the band structure [14]. This may be called the exciton mechanism of superconductivity [15].

3.1. The renormalization Z

At low frequency Z can be obtained from the self-energies and leads to the mass enhancement

$$Z(0) = 1 + \lambda = m^*/m, \qquad \lambda = -(\partial\Sigma/\partial\omega)_{\omega\to 0}. \tag{11}$$

The self-energy Σ is derived from the single-particle excitation energies including many-body effects [16]. To obtain the enhancement due to electron–phonon interaction it is assumed that Coulomb and band dressed effective mass, m_c, is known. We show in appendix A.1 that if both Fröhlich and $\boldsymbol{E}\cdot\boldsymbol{p}$ ep interactions are present

$$Z'(0) = m^{**}/m_c = (1+\lambda)(1+\lambda^{\mathrm{D}}) \tag{11a}$$

where λ and λ^{D} are the Fröhlich and $\boldsymbol{E}\cdot\boldsymbol{p}$ ep couplings, respectively.

In oxide superconductors where the exciton mechanism operates and the el interaction dominates, the effective mass increases sharply as the electron in motion carries with it a polaron cloud. This is discussed in appendix A.3 and used in section 6.

3.2. The pair field

To obtain the pair field $\phi(\omega)$ in equation (10) we need to obtain the ep, ee and el contributions to self-energy. The expressions for $\sum_{\mathrm{ep}}^{F}$ and $\sum_{\mathrm{ee}}^{O}$ are derived in many places like equations (3.21) and (5.14) in [2]. $\sum_{\mathrm{ep}}^{D}$ is obtained by replacing $g^{\mathrm{F}}_{kq\lambda}$ by $g^{\mathrm{D}}_{kKq\lambda}$ in $\sum_{\mathrm{ep}}^{F}$. This is shown in section 5. The effect of ee interaction is here tackled through an appropriate screening of the nuclear charge and is included in the ep interaction. The remaining el self-energy arising from electron–ion interaction can be expressed to second order as [15].

$$\sum_{\mathrm{el}}^{O} = \sum_{K} |\bar{V}_{k_{\mathrm{F}}}(K)|^2 G(k+K,\omega)$$

where

$$\bar{V}_{k_{\mathrm{F}}}(q) = \frac{V_{\mathrm{ei}}(q)}{\varepsilon(q,0)}\Gamma_0(k_{\mathrm{F}},q).$$

Here $V_{\mathrm{ei}}(q)$ is the Fourier transform of the bare electron–ion potential, $\Gamma_0(k_{\mathrm{F}},q)$ is the vertex function of the ee interaction and $\varepsilon(q,0)$ is the dielectric function of the electron gas [1]. The Green's function is given by

$$G^{-1}(k+K,\omega) = \omega - E_k - \sum_{K}\frac{|\bar{V}_{k_{\mathrm{F}}}(K)|^2}{E_k - E_{k+K}}.$$

This leads to band structure energy per ion as [14]

$$U_{\mathrm{bs}} = N^{-1}\sum_{k<k_{\mathrm{F}}}\sum_{K}{}' \frac{|\langle k+K|\bar{V}|k\rangle|^2}{E_k - E_{k+K}}$$

where N is the number of atoms and the prime indicates that $K = 0$ is excluded from the summation. Including the Darwin term

$$U_{\rm bs} = \sum_K{}' |S(K)|^2[\bar{V}^2(K) + \beta^2]\chi(K)\varepsilon(K) \tag{12}$$

where $\varepsilon(K)$ is the dielectric function and $\chi(q)$ is given by

$$\chi(q) = N^{-1}\sum_{k<k_{\rm F}}\left[\tfrac{1}{2}k^2 - \tfrac{1}{2}(k+q)^2\right]^{-1} = N_{\rm bs}(0)u(q/2k_{\rm F}) \tag{13}$$

$$u(x) = \frac{1}{2} + \frac{1-x^2}{4x}\ln\left|\frac{1+x}{1-x}\right|. \tag{13a}$$

Here $N_{\rm bs}(0)$ is the band structure electron density of states at the Fermi surface [6]. In the paired state the repulsive energy $\beta^2\chi(K)$ vanishes, giving the el contribution to the pair field ϕ in equation (10),

$$\phi_{\rm el} = F_{\rm bs}^{*2}\langle\beta^2\rangle\langle\chi(K)\rangle\langle\varepsilon(K)\rangle \tag{14}$$

$$F_{\rm bs}^{*} = \sum_{K<2k_{\rm F}+k_{\rm s}} n(K)|S(K)|^2. \tag{14a}$$

Here $F_{\rm bs}^{*}$ is the sum of all reciprocal lattice vectors that contribute to it and satisfy the condition $|K| < 2k_{\rm F} + k_{\rm s}$. Here $k_{\rm F}$ and $k_{\rm s}$ are the Fermi and Thomas–Fermi screening wavevectors respectively. $n(K)$ is the number of equivalent K vectors. This coupling arising due to electronic fluctuations (excitons) is discussed further in section 6.

4. Quenching of electron–ion $\boldsymbol{E}\cdot\boldsymbol{p}$ energy

We show that the interband scattering of a pair of electrons at the Fermi surface between two bands, one electron-like and the other hole-like, leads to a state for which the expectation value of the Darwin term vanishes.

Using the Born–Oppenheimer approximation we consider the nuclei 'clamped' in position as if these have infinite mass. Then we can write equation (2) as

$$H = H_{\rm e} + H_{\rm n}$$

with $H_{\rm n}$ as a small perturbation. On the basis of charge neutrality each unit cell will on an average contain a nucleus and two electrons. Following Hopfield [17] we take the screened electron–ion potential as a local symmetric potential concentrated in the unit cell. We treat the $\boldsymbol{E}\cdot\boldsymbol{p}$ term as a perturbation.

$$H = H_O + H' \tag{15}$$

$$H_O = \frac{p_1^2}{2m} + \frac{p_2^2}{2m} - \frac{z(x_1)e^2}{|x_1|} - \frac{z(x_2)e^2}{|x_2|} + \frac{e^2\,(x_{12})}{|x_{12}|} \tag{16}$$

$$H' = A\,\{\delta(x_1) + \delta(x_2)\} - A'\delta(x_{12}) \tag{17}$$

where

$$A = \frac{\pi}{2}\left(\frac{e^2\hbar^2}{m^2c^2}\right)z, \qquad A' = -\frac{\pi}{2}\left(\frac{e^2\hbar^2}{m^2c^2}\right). \tag{18}$$

We introduce the centre-of-mass and difference variables, $x = x_1–x_2$, $X = \frac{1}{2}(x_1 + x_2)$, and have

$$H_O = \frac{P^2}{2m^*} + \frac{p^2}{2\mu} - \frac{(z-0.25)e^{*2}}{|x|} \tag{19}$$

where $m^* = 2m$, $\mu = m/2$, $e* = 2e$

$$p = p_1 - p_2, \qquad P = \tfrac{1}{2}(p_1 + p_2). \tag{20}$$

Since the variables are separable the Schrödinger equation gives a wavefunction Ψ which is a product of a function $\Psi_1(x)$ of the internal coordinates, x and another function $\Psi_2(X)$ of the centroid's coordinate; X. $\Psi_1(x)$ describes the motion of a particle of mass μ, charge $-e^*$ and spin zero moving in a central field $V(x)$ of a charge $+(z-0.25)e^*$ and $\Psi_2(X)$ describes the motion of a free particle of mass m^*. We show later that $\Psi_1(x)$ refers to the momentum density and $\Psi_2(X)$ to the quantum phase of a superfluid.

The Bloch function $\Psi_k(x)$ in the unit cell in question can be represented as an expansion in spherical harmonics [17].

$$\psi_k(x) = \mathrm{e}^{\mathrm{i}K\cdot X}\sum_{l,m} Y_{lm}(\theta,\phi)g_{lmk}(x). \tag{21}$$

To estimate the $\boldsymbol{E}\cdot\boldsymbol{p}$ energy we use the pseudopotential theory and pick out the $l = 0$ component in equation (21). We expect the pseudo-wavefunction within the core to have no oscillation [14]. The pseudo-wavefunction has the form of a 1s hydrogen wavefunction with nuclear charge $\langle z - 0.25\rangle$. This is the approach taken by us in [7] to obtain empirically a T_c equation that gives the critical temperature of several metals and alloys.

In cell i, the wavefunction has the form

$$\Psi_K(x_i, X_i) = \mathrm{e}^{\mathrm{i}K\cdot X_i}g_{000}(x_i) \qquad g_{000} = (c^3/\pi)\exp(-cx_i) \tag{22}$$

$$c = \frac{z'}{a_H^* n^*}, \qquad a_H^* = \frac{\hbar^2}{\mu e^{*2}} = \frac{a_H}{2} \qquad n^* = 2n, \quad n = 1, 2, \ldots. \tag{23}$$

The contribution to energy by this component is

$$E_0 = -\frac{z'^2 e^{*4}\mu}{2n^{*2}\hbar^2} + \frac{\hbar^2 K^2}{2m^*}. \tag{24}$$

Here a_H is the Bohr radius. With this wavefunction and $x_i = x_{2i-1} - x_{2i}$ it can be shown [18] that

$$\langle\delta(x_{2i-1} - X_i)\rangle = \langle\delta(x_{2i} - X_i)\rangle = 8\langle\delta(x_{2i-1} - x_{2i})\rangle. \tag{25}$$

Then from equations (17) and (18)

$$H' = 16z'\,A'\delta(x_i). \tag{26}$$

We then have

$$H = H_0 + H' = \sum_{i=1}^{N/2}\left[\frac{P_i^2}{2m^*} + \frac{p_i^2}{2\mu} - \frac{z'e^{*2}}{|x_i|} + 16z'\,A'\delta\,(x_i)\right]. \tag{27}$$

H leads to a BCS type reduced Hamiltonian when the interaction potential is H'.

Consider the effect of the presence of two sections, one electron-like in band n and the other hole-like in band n', at the Fermi surface. These bands are centred about two different symmetry axes in the crystal such that

$$E_1(\boldsymbol{k}) = -E_2(\boldsymbol{k}') = -E_2\,(\boldsymbol{k} + \boldsymbol{K} + \boldsymbol{q}) \tag{28}$$

the positive sign describing the conduction band (electron section) and the negative sign the valence band (hole section). Here $\boldsymbol{q}$ is a phonon wavevector and $\boldsymbol{K}$ is a reciprocal lattice vector as shown in figure 1. A pair in an electron section centred at Γ is scattered to and fro to a hole section (band 2) centred at H of a square cross-section of the Brillouin zone;

$$(k\uparrow, -k\downarrow) \Leftrightarrow \left(k'\uparrow, -k'\downarrow\right) = (k + K + q\uparrow, -k - K - q\downarrow)\,. \tag{29}$$

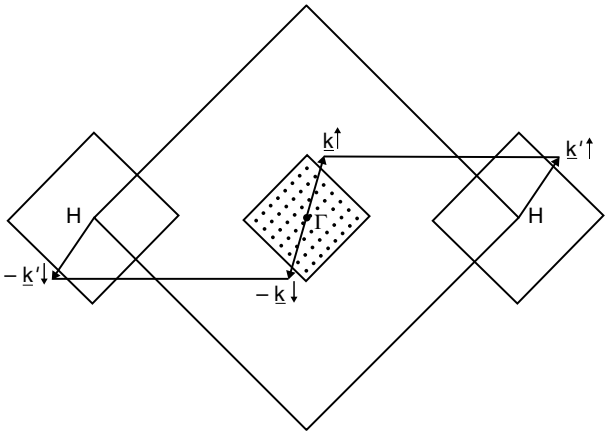

Figure 1. The square section of the Brillouin zone with an electron pocket centred at Γ and a hole pocket centred at H. A pair $(k\uparrow, -k\downarrow)$ from the electron section is scattered, to and fro, to the $(k'\uparrow, -k'\downarrow)$ state in the hole section. The electron section is shown dotted. The transition $|k\uparrow, -k\downarrow\rangle \Leftrightarrow |k'\uparrow, -k'\downarrow\rangle$ leads to a state in which the repulsive $\boldsymbol{E}\cdot\boldsymbol{p}$ energy vanishes, leading to an attractive interaction between the members of the pair. Here $k' - k = K + q$, where K is the reciprocal lattice vector and q is a phonon wavevector.

The $\boldsymbol{E}\cdot\boldsymbol{p}$ interaction perturbation can then have first order effect and the degeneracy is removed. The secular equation with $|1\rangle$ describing the electron and $|2\rangle$ the hole state,

$$|1\rangle = |k\uparrow, -k\downarrow\rangle, \qquad |2\rangle = |k'\uparrow, -k'\downarrow\rangle \qquad \text{and} \qquad |\psi\rangle = \alpha|1\rangle + \sqrt{(1-\alpha^2)}|2\rangle \tag{30}$$

is

$$\begin{pmatrix} 2\alpha^2(E_0+\Delta) - E & 2\alpha\sqrt{1-\alpha^2}\Delta \\ 2\alpha\sqrt{1-\alpha^2}\Delta & 2(1-\alpha^2)(E_0+\Delta) - E \end{pmatrix} = 0 \tag{31}$$

where $2(E_0 + \Delta) = \langle 1|H|1\rangle = \langle 2|H|2\rangle$ and $2\Delta = \langle 1|H|2\rangle$

There are two states with energies

$$E_{1,2} = [(E_0+\Delta) \pm \{(E_0+\Delta)^2 - 4\alpha^2(1-\alpha^2)(E_0^2 + 2\Delta E_0)\}^{1/2}] \tag{32}$$

for $\alpha = 1/\sqrt{2}$, $E_1 = E_0 + 2\Delta$ and $E_2 = E_0$.

So in state 2 the sum of ei and ee $\boldsymbol{E}\cdot\boldsymbol{p}$ energy vanishes in the condensed phase in which the pair of electrons continuously scatter from the e- to h-pocket. The hybridization of two degenerate wavefunctions $|1\rangle$ and $|2\rangle$ in the electron and hole sections of the Fermi section with energy $(E_0 + \Delta)$ removes the degeneracy and produces a bonding state with energy E_0 and an antibonding state with energy $(E_0 + 2\Delta)$, respectively. As $(E_0 + \Delta)$ is the chemical potential quenching produces an energy gap, $E_g = 2\Delta$, around the Fermi surface.

The formation of a state of a lower energy in the superconducting compared to the normal phase through the scattering of the pairon from the electron to the hole pocket at the Fermi surface explains the property of 'off-diagonal long-range order' of the BCS wavefunction discovered by Yang and described in [19]. We write a solution of the one-pairon wave equation from equation (19) as

$$H\phi_k(x) = \varepsilon_k\phi_k(x)$$

where $\phi_k(x)$ is expressed as a Wannier function

$$\phi(x - X_i) = (N/2)^{-1/2}u_0(x)\sum_k \mathrm{e}^{\mathrm{i}k\cdot(x-X_i)}. \tag{33}$$

Following Ambegaokar [19] the field operator

$$\psi^{+}(x) = \sum_{k} c^{+}_{k\uparrow} c^{+}_{-k\downarrow} \phi^{*}_{k\uparrow}(x_1)\phi^{*}_{-k\downarrow}(x_2)$$

is used to express the N-particle BCS wavefunction (un-normalized) as

$$\psi_{0N} = \left[\int \mathrm{d}^3x_1\, \mathrm{d}^3x_2 \phi(x_1 - x_2)\psi^{+}_{\uparrow}(x_1)\psi^{+}_{\downarrow}(x_2)\right]^{N/2} |0\rangle = \left[\sum_{k} \phi(k) c^{+}_{k\uparrow} c^{+}_{-k\downarrow}\right]^{N/2} |0\rangle$$

where

$$\phi(k) = \left(\frac{N}{2}\right)^{-1/2} \int \mathrm{d}^3x_1\, \mathrm{d}^3x_2\, u^{*}_0(x_1)u^{*}_0(x_2)\delta(x_1 - x_2)u_0(x_1)u_0(x_2) \sum_{n} \mathrm{e}^{\mathrm{i}k\cdot x_n}.$$

Using a variational BCS wavefunction

$$\psi = \prod_{\substack{k,k' \\ k\neq k'}} \left(u^2_k + v^2_k b^{+}_k\right)\left(u^2_{k'} + v^2_{k'} b^{+}_{k'}\right) |0\rangle \tag{34}$$

the BCS reduced Hamiltonian for a two-band model is

$$H_{\mathrm{red}} = \sum_{k} \varepsilon_k b^{+}_k b_k + \sum_{k'} \varepsilon_{k'} b^{+}_{k'} b_{k'} - \sum_{k'\neq k} V_{kk'} b^{+}_{k'} b_k \tag{35}$$

where $k' - k = K + q$ with k and k' belonging to electron and hole sections, respectively, and

$$V_{kk'} = \langle k'n' | H' | kn\rangle \tag{36}$$

n' and n being the band indices of the hole and electron section. For a single pairon with

$$u_k = v_k = u_{k'} = v_{k'} = 1/\sqrt{2} \tag{37}$$

the expectation value of energy in the ground state with $V_{kk'} = 2\Delta$ is

$$E = 2(E_0 + \Delta) - 4V_{kk'} u_k v_k u_{k'} v_{k'} = 2E_0.$$

As in equation (32) the quenching is complete for $\alpha = 1/\sqrt{2}$, that is when the pairon spends equal time in the electron and hole sections. From BCS theory equation (37) holds only for a pairon at the Fermi surface and is a consequence of the variational nature of the BCS wavefunction. If $\alpha \neq 1/\sqrt{2}$, from equation (32) the quenching is incomplete. We define the super electron charge density per atom as

$$n_{\mathrm{s}} = 2\alpha(1 - \alpha^2)^{1/2} \tag{38}$$

α depends on several factors like crystal structure, $K_{\min}/2k_{\mathrm{F}}$ ratio etc and even at the Fermi surface may be different from $1/\sqrt{2}$, contrary to the BCS model. This is discussed in section 6, where n_{s} is different from unity for many oxide superconductors.

The wavefunction for H_{red} (equation (35)) as a projection of $|\psi_0\rangle$ on the N-particle space can be expressed in coordinate representation as

$$\begin{aligned}\psi_{0N}(x_1s_1, x_2s_2, \ldots, x_Ns_N) = {} & \exp\left[\mathrm{i}K\cdot\left\{X_1 + X_2 + \cdots + X_{N/2}\right\}\right] \\ & \times A\phi(x_1 - x_2)\,\chi(1\uparrow, 2\downarrow)\,\phi(x_3 - x_4)\,\chi(3\uparrow, 4\downarrow) \\ & \cdots\phi(x_{N-1} - x_N)\,\chi(N-1\uparrow, N\downarrow)\end{aligned} \tag{39}$$

where K and ϕ are the same for all pairs and the operator A antisymmetrizes the entire function. This is the wavefunction with finite momentum density of the superfluid. It can be expressed as $\sqrt{\rho}\exp(\mathrm{i}\eta)$ with ρ representing the density and η the quantum phase of the superfluid providing justification for the basic assumptions of the Ginzburg–Landau equations [20]. As we are concerned with critical temperature we shall not pursue many aspects of superconductivity associated with non-vanishing K and take $K = 0$.

5. Self-energy of the super state and the T_c equation

The self-energy in equation (9) for a dirty superconductor has only the component τ_4, that gives the normal self-energy, $\xi(\omega) = [1 - Z(\omega)]\omega$, and the component τ_1, that gives the pairing self-energy, $\phi(\omega)$. In the present model $\phi(\omega)$ is obtained from H' in equation (27) and the renormalization factor $Z(\omega)$ for low frequencies is discussed in section 3.1 and appendix. The T_c equation is obtained solving these equations simultaneously at the critical temperature [6].

Consider a pairon centred at X_j in electron band γ in state $|1\rangle = |\underline{k}_1\uparrow, -\underline{k}_1\downarrow\rangle$ scattered to state $|2\rangle = |\underline{k}_2\uparrow, -\underline{k}_2\downarrow\rangle$ in hole band δ. The wavefunction can be expressed as in equation (33),

$$\phi\left(\underline{x} - \underline{X}_j\right) = (N/2)^{-1/2}\, u_0(x) \left\{ \alpha \sum_{\underline{k}_1 \epsilon \gamma} \mathrm{e}^{\mathrm{i}\underline{k}_1 \cdot (\underline{x} - \underline{X}_j)} + \sqrt{1-\alpha^2} \sum_{\underline{k}_2 \epsilon \delta} \mathrm{e}^{\mathrm{i}\underline{k}_2 \cdot (\underline{x} - \underline{X}_j)} \right\}. \tag{40}$$

The transition from γ to δ and back to γ takes place through emission and absorption of a phonon of momentum of $\hbar(\underline{k}_1 - \underline{k}_2)$ and energy $\hbar^2(\underline{k}_1^2 - \underline{k}_2^2)/2m^*$ between the pairon and the nucleus at $\underline{X}_j$ through H' interaction. The transition probability for a one-phonon process has been discussed by Glauber [21] for neutron scattering and can be used for the pairon scattering as both have delta function scattering potentials and energy and momentum transfers for both are in the range of the lattice frequencies and wavevectors. We obtain

$$W(k, \Omega) = \frac{8\pi^3\hbar^3}{Mm^{*2}} \left| b_j \mathrm{e}^{\mathrm{i}\underline{k}\cdot\underline{X}_{0j}} \mathrm{e}^{-q\cdot\underline{X}_{0j}} \right|^2 \times \sum_{n_i, n_f, \lambda} w\left(n_f, n_i\right) \left| \langle n_f | \, k \cdot \epsilon_{q\lambda} Q_{q\lambda} | n_i \rangle \right|^2 \mathrm{e}^{-2B} \delta\left[\hbar^2 k^2/2m^*, \hbar\Omega\right] \tag{41}$$

where we have used H' in the scattering length, b $(=z'e^{*2}/\mu c^2)$ approximation,

$$H' = \frac{\pi}{2}\left(\frac{z'e^2\hbar^2}{m^2c^2}\right) 16\delta(x) = \frac{2\pi\hbar^2}{m^*} b\delta(x). \tag{42}$$

In equation (41) M is the mass of the nucleus, m^* is the mass of the c.m. of the pairon, $w(n_f, n_i)$ is the probability of finding the lattice in the initial state E_i and final state E_f, and

$$k = k_1 - k_2 = \boldsymbol{K} + \boldsymbol{q} \tag{43a}$$

$$\frac{\hbar^2 k^2}{2m^*} = \hbar\Omega_{q\lambda}. \tag{43b}$$

Here $\boldsymbol{K}$ is a reciprocal lattice vector and $\boldsymbol{q}$ a phonon wavevector, $\epsilon_{q\lambda}$ is the unit polarization vector and $Q_{q\lambda}$ is the Fourier component of the displacement vector in the normal modes,

$$Q_{q\lambda} = \left(\frac{\hbar}{2\Omega_{q\lambda}}\right)^{1/2} \phi_{q\lambda}$$

where $\phi_{q\lambda}$ is defined in equation (7). e^{-2B} is the Debye–Waller factor. As discussed earlier the scattering produces bonding and antibonding states (equation (32)) with energies $\pm\Delta$ about the Fermi level. This can be expressed it in terms of scattering length, $b_+ = +b$ and $b_- = -b$.

We now show that equation (42) gives the pairing self-energy which is similar to that obtained as the solution of Eliashberg equations [6]. The coherent inelastic scattering of pairons by the nucleus bound in the solid through the recoilless process produces the pairing self-energy and the bonding and antibonding states. On the other hand, the incoherent scattering produces the non-bonding state and the normal state self-energy. The inelastic incoherent cross section for neutron scattering for the one-phonon process based on equation (41) has been obtained by Placzek and van Hove [22]. We use it to obtain the transition probability for the incoherent pairon scattering by the nucleus including the following features that apply to the present case:

(i) the virtual scattering process $|1\rangle \Leftrightarrow |2\rangle$ takes place above the Fermi sea amongst available states within $\pm h\omega_{\mathrm{D}}$ of the Fermi surface,

(ii) in the super state for a uniform isotropic superconductor the electron density of states is $N(0)\,\mathrm{Re}\,\{\omega/\sqrt{\omega^2-\Delta^2(\omega)}\}$, where $N(0)$ is the density of states at the Fermi surface and $\Delta(\omega)$ is the gap field.

These are required to get $w\ (n_f, n_i)$ in equation (41).

We obtain following reference [22] the transition probability for one-phonon inelastic incoherent scattering,

$$W(\omega) = \frac{8\pi^3\hbar^3}{m^{*2}}\left\{\langle b^2\rangle - \langle b\rangle^2\right\}\sum_{K<2k_{\mathrm{F}}+q_{\mathrm{D}}}\iint \mathrm{d}\omega'\,\mathrm{d}\Omega\, S(\omega', \Omega, \omega) \tag{44}$$

where

$$S(\omega', \Omega, \omega) = \frac{(K+q)^2}{2M\Omega_{q\lambda}}\frac{N(0)}{(4\pi)^2}\mathrm{Re}\left(\frac{\Delta(\omega')}{\sqrt{\omega'^2-\Delta^2(\omega)}}\right)$$
$$\times\,[\exp(-2B)\left\{D_q(\omega'+\omega) + D_q(\omega'-\omega)\right\}F(\Omega). \tag{45}$$

Here the phonon propagator $D_q(\omega) = (\omega - \Omega - \mathrm{i}o)^{-1}$ is the same as obtained in the expression for self-energy of the super state using the Eliashberg equation in [12] and $F(\Omega)$ is the phonon density of states. From equation (6)

$$\langle 1|\,H'\,|2\rangle = 2\beta = 16\beta'. \tag{46}$$

The ensemble averages, $\langle b^2\rangle$ and $\langle b\rangle^2$, can be expressed in terms of the average over β. The Ω dependent part of S in equation (45) can be expressed in terms of the electron–phonon coupling constant g^{D} in equation (4)

$$\alpha^2F(k, \Omega) = 2\sum_j N(0)\left|g^{\mathrm{D}}_{kj}\right|^2\delta(\Omega - \omega'_{kj}) \tag{47}$$

where

$$g^{\mathrm{D}^2}_{kj} = \left(\frac{\hbar}{2M\omega'_{kj}}\right)\langle|K+q|^2\rangle\left\{\langle\beta^2\rangle - \langle\beta\rangle^2\right\}. \tag{48}$$

The summation over K and q can be expressed in terms of F^*_{bs} defined in equation (14*a*). On account of inversion symmetry K and q always appear in pairs $\pm K$, $\pm q$. For a single scattering event, the two are independent and $\boldsymbol{q}$ depends on the shape of the electron and hole pockets (figure 1). The recoil corresponds to two displaced probability density functions, one for emission and the other for absorption. The total number of possibilities is then given by $(2F^*_{\mathrm{bs}})^2$. We can write

$$\lambda = 2\int\frac{\alpha^2(\Omega)F(\Omega)\,\mathrm{d}\Omega}{\Omega} = \frac{N(0)\left\langle g^{D^2}\right\rangle}{M\left\langle\Omega^2\right\rangle} \tag{49}$$

where

$$\left\langle g^{\mathrm{D}^2}\right\rangle = \frac{F^{*2}_{\mathrm{bs}}\left\langle|K+q|^2\right\rangle\left\{\left\langle\beta^2\right\rangle - \langle\beta\rangle^2\right\}}{2} \tag{50}$$

with

$$F^*_{\mathrm{bs}} = \sum_{K<2k_{\mathrm{F}}+q_{\mathrm{D}}} n(K)\,|S(K)|^2. \tag{51}$$

The average over $\langle\Omega^{-2}\rangle$ in equation (49) is over frequencies of the harmonic oscillator associated with the nucleus and the pairon and can be expressed as

$$\langle\Omega^{-2}\rangle = \langle\Omega^{-1}\rangle_{\text{lattice}} \cdot \langle\Omega^{-1}\rangle_{\text{pairon}}. \tag{52}$$

It is easily shown that for a Debye solid at $T = 0$ K [23]

$$\langle\Omega^{-1}\rangle_{\text{lattice}} = (\tfrac{2}{3}\omega_{\text{D}})^{-1}. \tag{53a}$$

The lattice waves that are involved in the pairon scattering $|1\rangle \leftrightarrow |2\rangle$ are from s to s state at the Fermi surface so the density of phonon states is reduced by a factor $N_{\text{s}}(0)/N(0)$, where $N_{\text{s}}(0)$ is the s-electron density of states. We obtain

$$\left\langle\Omega^{-1}\right\rangle_{\text{pairon}} = \frac{N(0)}{N_{\text{s}}(0)} \int_0^{(2/3)\omega_{\text{D}}} \frac{F(\Omega)\,\mathrm{d}\Omega}{\Omega} = \frac{N(0)}{N_{\text{s}}(0)} \left(\frac{3}{2}\omega_{\text{D}}\right)^{-1}. \tag{53b}$$

From equations (49), (52) and (53),

$$\lambda = \frac{N^2(0) F_{\text{bs}}^{*2} \left\langle |K+q|^2\right\rangle \left\{\left\langle\beta^2\right\rangle - \langle\beta\rangle^2\right\}}{2N_{\text{s}}(0) M\omega_{\text{D}}^2} \tag{54}$$

with $N_{\text{s}}(0)\beta \sim n_{\text{s}}$ defined in equation (38).

For coherent scattering we obtain a similar expression except that $\langle\beta\rangle^2$ is small compared to $\langle\beta^2\rangle$ by a factor $N_{\text{s}}(0)/N(0)$ as the former involves s to s scattering while the latter from s to any other state, s, p, d, . . ., at the Fermi surface. For the inelastic coherent scattering we then obtain

$$\lambda^{\text{D}} = \frac{N(0) F_{\text{bs}}^{*'2} \left\langle |K|^2\right\rangle \left\langle\beta^2\right\rangle}{2M\omega_{\text{D}}^2} \tag{55}$$

where

$$F_{\text{bs}}^{*'} = \sum_{K<2k_{\text{F}}} n(K)\,|S(K)|^2 \tag{55a}$$

Equations (55) and (55*a*) are in fact obtained in the 'incoherent approximation', in which one averages the scattering over a large number of Brillouin zones and over a large number of angles when the specific effects of coherence are eliminated [24]. In this case the effect of phonon wavevector $\boldsymbol{q}$ in the summation in equation (55*a*) vanishes and is the same as in elastic Bragg scattering.

We now consider the case when the pairon enters the core of the ion in equation (19). The electron–ion interaction weakens and may even vanish due to the cancellation theorem [14]. However, the ee field due to higher energy cut-off would still exist. The pseudopotential for the pairon can then be expressed as

$$\begin{aligned} V(x) &= +\frac{(z-0.25)\,e^*}{x} \qquad x \geqslant 2R \\ &= -\frac{0.25e^*}{x} \qquad x < 2R \end{aligned} \tag{56}$$

where R is the radius of the core. In the core region $V(x)$ is repulsive but the $\boldsymbol{E}\cdot\boldsymbol{p}$ interaction is attractive. Hence Cooper pairing that makes it vanish is opposed in this region. In this case the ee coupling is given by equation (54) if we replace z in β in equation (6) by -0.25. This is equivalent to the pseudopotential μ^* of Morel and Anderson [25]. Since $N_{\text{s}}(0)\beta \sim n_{\text{s}}$, which does not change, we have

$$\mu^* = \left(-\frac{0.25}{z-0.25}\right) \frac{N^2(0) F_{\text{bs}}^{*''2} \left\langle |K+q|^2\right\rangle \left\{\left\langle\beta^2\right\rangle - \langle\beta\rangle^2\right\}}{2N_{\text{s}}(0) M\omega_{\text{D}}^2} \tag{57}$$

where

$$F_{\mathrm{bs}}^{*''} = \sum_{K<2k_{\mathrm{F}}+k_{\mathrm{s}}} n(K)\left|S(K)^2\right|. \tag{58}$$

In equation (58) k_{s} is the Fermi–Thomas screening wavevector.

To obtain $\phi(\omega)$, the pairing self-energy, we perform the integration over ω' in equation (44) expressing that over Ω as λ, λ^{D} and μ^* in equations (54), (55) and (57), and at T_{c} equate it to $\xi(\omega)$,

$$\begin{aligned} I = \phi(\omega)_{T=T_{\mathrm{c}}} &= \Delta_0\left[\int_0^{\omega_{\mathrm{c}}} \frac{\mathrm{d}\omega'}{\omega'}\tanh\left(\frac{\omega'}{2T_{\mathrm{c}}}\right)\times\left[\lambda-\lambda^{\mathrm{D}}-\mu^*\right]\right] \\ &= \Delta_0\left[\ln\left(\omega_{\mathrm{c}}/T_{\mathrm{c}}\right)\right]\left[\lambda-\lambda^{\mathrm{D}}-\mu^*\right] \\ &= 2\pi\hbar W^{\mathrm{inc}}(\omega) \\ &= \xi(\omega)_{T=T_{\mathrm{c}}} = Z(0)\Delta_0. \end{aligned} \tag{59}$$

Using equation (11*a*) and $\omega_{\mathrm{c}} = (2/3)\omega_{\mathrm{D}}$ we obtain

$$T_{\mathrm{c}} = \frac{\theta_{\mathrm{D}}}{1.5}\exp\left[-\frac{(1+\lambda)(1+\lambda^{\mathrm{D}})}{\lambda-\mu^*-\lambda^{\mathrm{D}}}\right]. \tag{60}$$

This is McMillan's experimentally adjusted T_{c} equation with minor differences. The orders of magnitude of λ, λ^{D} and μ^* are 1, 0.04 and 0.1 respectively [6]. We show later that these values are obtained from equations (54), (55) and (57) when appropriate values of the materials parameters, $N(0)$, F_{bs}^*, β and θ_{D} are substituted in these equations.

The exponential factor in equation (60) can be interpreted as the fraction of collisions with recoil in pairon scattering by the nucleus using Lipkin's sum rule [13]. In equation (41) the probability function $w(n_f, n_i)$ satisfies the condition

$$\sum_{n_f} w(n_f, n_i) = 1$$

where

$$w(n_f, n_i) = \left|\langle n_f|\exp(\mathrm{i}k\cdot X_j)\,|n_i\rangle\right|^2.$$

Lipkin's sum rule gives

$$\langle\hbar\Omega\rangle\sum_{n_f\neq n_i} w(n_f, n_i) = (\hbar k)^2/2M = R \tag{61}$$

where R is the free recoil energy of the nucleus and as shown in equation (53*a*)

$$\langle\Omega\rangle = (2/3)\omega_{\mathrm{D}}.$$

We obtain

$$\sum_{n_f\neq n_i} w(n_f, n_i) = \frac{R}{(2/3)\omega_{\mathrm{D}}} = 1 - \sum_{n_i} w(n_i, n_i). \tag{62}$$

But the sum of $w(n_i, n_i)$ is the recoilless fraction that gives $\exp(-2B)$, the Debye–Waller factor with

$$2B = \langle K^2\rangle\langle u^2\rangle. \tag{63}$$

The result in equation (62) is obtained for $T = 0$. As T increases R increases due to increase in the number of phonons,which increases the fraction of scattering events with recoil and hence decreases the fraction of recoilless collisions. For a one-phonon process

Table 1. The parameters used to obtain the critical temperature, T_c, from equation (65) for comparison with experiment. The values used for K_s and χ_p to obtain β using equation (67) are from [27]. z is the valence used in equation (67) to obtain β. The values of $N(0)$, λ, θ and T_c are from [6]. F^*_{bs} is calculated from Fermi surface studies for Pb (see text) but for all others from $K < 2k_F$ and best fit to T_c. Note that to estimate β for Pb z is taken here as two and not four to fit the results in agreement with [7].

Element	z	K_s (%)	χ_p ($\times 10^6$ emu mol^{-1})	β (meV)	$N(0)$ (states eV^{-1})	λ [6]	θ_D (K)	F^*_{bs}	$\langle\|K+q\|^2\rangle$ (Å^{-1})	λ^D (cal)	T_c (K) (obs)	T_c (K) (cal)
V	5	0.57	133	4.84	1.31	0.60	399	30	4.55	0.020	5.3	5.22
Nb	5	0.89	109	9.20	0.91	0.82	277	30	4.18	0.047	9.22	8.69
Ta	5	1.1	8.3	14.93	1.04	0.65	258	18	4.24	0.087	4.48	5.39
Mo	2	0.59	25.6	10.25	0.28	0.41	460	18	4.28	0.0023	0.92	0.71
W	2	1.04	16.0	30.85	0.148	0.29	396	18	4.36	0.0084	0.012	2.22
Al	3	0.161	18.7	5.87	0.208	0.38	428	26	3.64	0.0036	1.16	1.04
Pb	2	1.46	43	15.11	0.30	1.12	105	26	3.63	0.075	7.19	5.22
In	3	0.81	23	24.02	0.212	0.71	112	14	2.61	0.032	3.40	2.36

the recoilless fraction vanishes rapidly as T approaches $T_c = R/k_B$, as in the Mossbauer effect [26]. Comparing equations (55) and (63), $2B$ is λ^D, and equating R to $k_B T_c$ we obtain

$$T_c = \frac{\theta_D}{1.5}\lambda^D = \frac{\theta_D N(0)\langle\beta^2\rangle F^{*2}_{bs}\langle|K|^2\rangle}{3M\omega_D^2}. \tag{64}$$

Expressing T_c and θ_D in K, $N(0)$ in states eV^{-1}, β in meV, M in amu, $K+q$ in Å^{-1},

$$\begin{aligned} T_c(\mathrm{K}) &= 0.186\,\frac{N(0)\langle\beta^2\rangle F^{*^2}_{bs}\langle|K+q|^2\rangle}{M\theta_D} \\ &= 0.667\,\lambda^D\theta_D. \end{aligned} \tag{65}$$

In table 1 we give T_c obtained from equation (65) with estimates of β from the Knight shift,

$$K_s = \frac{8\pi}{3}\chi_p\langle|u_k(0)|^2\rangle_{FS} \tag{66}$$

$$\beta = \frac{\pi}{2}\left(\frac{e^2\hbar^2}{m^2c^2}\right)z'\langle|u_k(0)|^2\rangle_{FS} = 0.75\,\mu_B^2(z-0.25)\frac{K_s}{\chi_p}. \tag{67}$$

Here χ_p is the nuclear magnetic susceptibility and $\langle|u_k(0)|^2\rangle_{FS}$ is the average s-electron density at the nucleus for the states at the Fermi surface. The values of K_s and χ_p are taken from [27].

For fcc Pb, $k_F = 1.57$ Å^{-1}, $q_D = 1.25$ Å^{-1} and $a = 4.94$ Å. The weight of the reciprocal lattice vectors satisfying the condition $|K| < 2k_F$ is 26. The way these reciprocal lattice vectors produce non-vanishing contribution to the pair field is illustrated in figure 2 by the [110] section of the FS of Pb as given by Anderson and Gold [28]. $\Psi_{[110]}$ is a hole orbit centred at Γ in the second zone and $\zeta_{[110]}$ are six electron orbits in the third zone centred at $K, U, \ldots,$ points in the Brillouin zone. A pair $|1\rangle$ gets scattered to $|2\rangle$ from the hole to the electron section such that $\boldsymbol{k}' - \boldsymbol{k} = \boldsymbol{K}(220) + \boldsymbol{q}$, where $\boldsymbol{q}$ is a phonon vector. We call $K(220)$ active. On this basis only 26 reciprocal lattice vectors in Pb are active. The values of F^*_{bs} in table 1 are those that satisfy the condition $|K| < 2k_F$ and give values close to T_c as detailed studies of the Fermi surface were not made.

The agreement of T_c obtained from equation (65) with parameters given in table 1 for all the elements is satisfactory except for W, where the estimate of β appears incorrect. The Knight shift in this case may not all be due to the contact term alone.

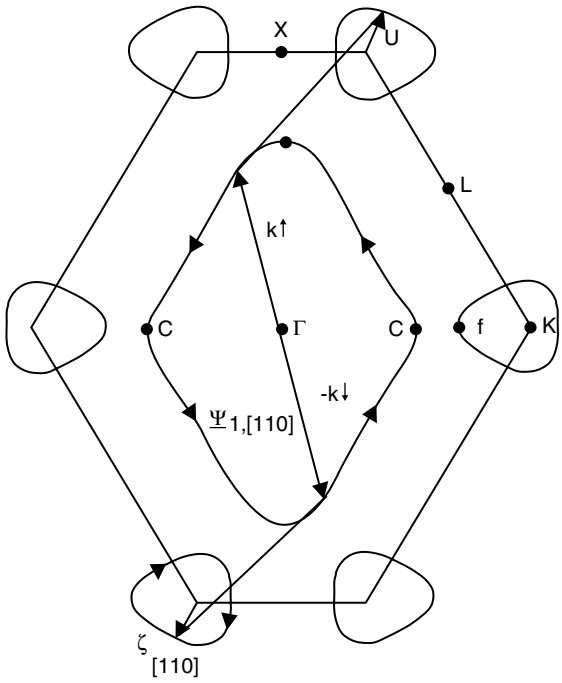

Figure 2. The [110] section of the Fermi surface of Pb as given by Anderson and Gold [28]. The $\psi_{[110]}$ is a hole orbit centred at Γ in the second zone and $\varsigma_{[110]}$ are six electron orbits in the third zone centred at K, U, ... points in the Brillouin zone. A pair $(k\uparrow, -k\downarrow)$ gets scattered to and fro, from the hole to the electron state $(k'\uparrow, -k'\downarrow)$ such that $k' - k = \boldsymbol{K}(220) + \boldsymbol{q}$ where $\boldsymbol{q}$ is a phonon wavevector.

5.1. Criterion for superconductivity

From equation (65) the criterion for superconductivity to exist can be obtained and is as follows.

(1) The minimum reciprocal lattice vector $K_{\min}$ should satisfy $K_{\min}/2k_{\mathrm{F}} < 1$.
(2) Even if condition (1) is satisfied there have to be electron and hole pockets in different bands at the Fermi surface to obtain non-vanishing values of F^*_{bs}.

We illustrate the applicability of these rules with some examples.

With $z = 1$, the Fermi surface does not cut the zone boundary so superconductivity does not occur in alkali and noble metals at normal pressure. Amongst group IIA and IIIA elements in the periodic table only Be and La are superconductors. In the double-zone hcp scheme in Be, from [29], it is seen that the presence of the $h_2(\Gamma)$ coronet and the $e_3(\mathrm{K})$ cigar shaped pocket makes $F^*_{\mathrm{bs}} \neq 0$. Likewise, in La $h_5(\Gamma\mathrm{A})$ and $e_7(\mathrm{HK})$ form the conjugate sections. In all the rest of the elements in these groups the presence of a multiply connected hole or electron section makes F^*_{bs} vanish.

In 3d metals Cr to Ni and in 4d metal Pd magnetic interactions make degenerate time-reversed pair states at the Fermi surface non-degenerate so F^*_{bs} vanishes. In other cases T_{c} is directly proportional to $N(0)$ in the transition metal elements, in contrast to the BCS result, that gives exponential dependence.

There are several metals like Cs, Sc and Y which do not superconduct at normal pressure but do so under high pressure. In these cases, F^*_{bs} changes from zero to non-zero values at high pressure. For example, caesium shows superconductivity at high pressure of 120 kbar

with T_c of 1.5 K. Analysis of the electronic structure of Cs with pressure shows [30] that at normal pressure there is a single band below the Fermi surface. It is only when the cell volume, V, decreases to less than half its volume at normal pressure, $V_0(V/V_0 = 0.4)$, that a second band appears below the Fermi surface at X_3. This occurs at the pressure of 43 kbar. But the contribution of band 2 to the total charge is only 2%. So the charge distribution is mainly that of the first band. Superconductivity occurs at 120 kbar when e- and h-sections have comparable charge densities (see equation (38)).

The band structure of A15 compounds has been studied by Mattheiss [31]. He finds that as many as 15 Fermi surface sheets exist in this structure. This enhances F^*_{bs} and hence T_c. For example, consider Nb_3Sn. For Nb, $F^*_{bs} = 30$ (table 1) is obtained from (110), (200) and half of (210). In Nb_3Sn another half of (210) is added, making $F^*_{bs} = 42$. Then T_c (Nb_3Sn) = T_c (Nb) $\times (42/30)^2 = 18.07$ K. On a similar basis, T_c (V_3Si) = T_c(V) $\times (54/30)^2 = 17.2$ K. In both cases the agreement with experiment is good, indicating that Sn and Si atoms may not play any significant role in the superconductivity of these A15 compounds.

5.2. *Isotope effect*

Equation (65) suggests that $T_c \propto (M\theta_D)^{-1} \propto M^{-1/2}$. The Darwin term energy is also dependent on the isotopic variation of an atom as the radius of the nucleus varies with atomic number as $A^{1/3}$ and $\delta(0)$ depends on the electron charge density at the nucleus.

Consider $T_c \propto M^{-\delta}$, $(M\theta_D)^{-1} \propto M^{-0.5}$, and $\beta \propto M^{+\varepsilon}$. This gives

$$\delta = 0.5(1 - 4\varepsilon) \tag{68}$$

where

$$\varepsilon = (M/\beta)(\partial\beta/\partial M) \tag{69}$$

δ can account for the deviation of isotope effect coefficient from 0.5.

5.3. *The Coulomb pseudopotential, μ^**

We obtain values of λ and μ^* from tunnelling experiments. These can be compared using equations (54) and (57),

$$\left|\frac{\lambda}{\mu^*}\right| = \frac{z - 0.25}{0.25}\,\frac{F^{*2}_{bs}}{F^{*''2}_{bs}}. \tag{70}$$

For Pb, $k_F = 1.57$ Å^{-1}, $q_D = 1.25$ Å^{-1}, and $k_s = 1.95$ Å^{-1}. Then $F^*_{bs} = 50$, $F^{*'}_{bs} = 26$, and $F^{*''}_{bs} = 62$. With $z = 4$ and $\lambda = 1.12$, $\mu^* = 0.12$, which agrees with experiment [6].

5.4. *Estimates of λ*

The T_c equations in (60) and (64), despite their vastly different forms, represent the same physical fact: the coherent recoilless scattering of pairons by the nucleus provides the binding energy between the members of the pair through quenching of the repulsive electron–ion $\boldsymbol{E}\cdot\boldsymbol{p}$ interaction energy. The sum of the fraction with recoil, $\exp[-\frac{(1+\lambda)(1+\lambda^D)}{\lambda-\mu^*-\lambda^D}]$, and without recoil, $\exp(-\lambda^D)$, is always unity. Through Lipkin's sum rule [13] we then obtain both equations (60) and (64). From equations (54) and (55)

$$\frac{\lambda}{\lambda^D} = \frac{N(0)}{N_s(0)}\,\frac{\{\langle\beta^2\rangle - \langle\beta\rangle^2\}}{\langle\beta\rangle^2}\,\frac{F^{*2}_{bs}}{F^{*'2}_{bs}} \sim f\frac{\theta_D}{T_c}. \tag{71}$$

This is obtained on the basis that incoherent and coherent scattering probabilities are nearly proportional to θ_D and T_c, respectively. From table 1, the experimental value of f is V (0.4), Nb (0.6), Ta (0.13), Mo (0.36), Al (0.29), In (0.67) and Pb (1.0).

6. Exciton mechanism—superconductivity in oxides

In ionic crystals with sizable density of electrons in the conduction band there is screening of the pseudopotential which for a free electron gas can be expressed as the Lindhard dielectric function. Schrieffer [1] has shown that the spectral function of these excitations is of the same form as the spectral function of the phonon Green's function except that the weight function in the former involves matrix elements of the electronic density fluctuations while in the latter that of the ionic density fluctuation operator. Since the excitations are electronic these are called excitons. Our interest is in the scattering of pairon from a hole to an electron band with a momentum transfer $k'-k = K+q = q'$ where q' is the momentum of the exciton. We need the screening factor $\varepsilon(q')$ for the electron–ion pseudopotential

$$\varepsilon(q') = \left[1 - 8\pi e^2/\Omega_a q'^2\right]\chi(q')$$

where $\chi(q')$ is defined in equation (13) and Ω_a is the atomic volume.

The coupling constant, ζ, can be obtained using equation (14),

$$\zeta = N_s(0)\phi_{el} = N_s(0)\langle\beta^2\rangle F_{bs}^{*2}\,\langle\chi(K)\rangle\,\langle\varepsilon(K)\rangle\,. \tag{72}$$

On comparison with equations (49) and (50) we note that the factor $\langle\chi(K)\rangle\langle\varepsilon(K)\rangle$ of the exciton coupling is equivalent to the $\langle|K+q|^2\rangle/2M\langle\omega_{k\lambda}^2\rangle_D$ of the phonon coupling. In oxide superconductor the charge carriers exist in the (Ba/Sr)–O plane and are coupled to the stretching mode B_{1g} vibrations of the apical oxygen in the M^{+n}–O4–Cu2 bond [32]. The carrier concentration, n_s, is determined by the vibrations of the O4 atoms which appear as a doublet along the z connected by inversion and have value close to unity for the optimally doped samples. Consequently, the charge carriers are polaronic, which we have shown through the analysis of the results of photoemission and femtosecond optical absorption spectroscopy [32]. Maxim *et al* [33] have given a similar model and have also given experimental support for it. In this case there are two lattice vectors that connect hole pocket at $\pm(1/2, 1/2, 0)$ to the electron pocket at $\pm(0, 1, 0)$, so $F_{bs}^* = 2$. Further, from equation (13) $\chi(q') = N_{bs}u(x)$, $x = q'/2k_F = \sqrt{5/8}$. Taking $N_{bs} = N(0)/(m^{**}/m^*)$ where $N(0)$ is the free electron density of states, $N(0) = 0.75\,z'/E_F$, with $E_F = \hbar\,\omega_{ex,max}$ and $z' = 1$ ($Ba^{2+}O^{1-} \leftrightarrow Ba^{2+}O^{2-} + e^+$) we obtain T_C using steps similar to the derivation of the equation (64). Taking $\langle\omega_{ex}^2\rangle^{1/2} = (2/3)\omega_{ex,max}$ and $N_s(0)\,\beta = n_s$,

$$k_B T_c = \zeta\,\hbar\left\langle\omega_{ex}^2\right\rangle^{1/2} = \frac{1}{3}\,F_{bs}^{*2}\frac{n_s\beta}{m^{**}/m^*} \tag{73}$$

where m^{**} is the exciton-dressed mass of the pairon whose undressed mass is m^* (equation (19)).

Expressing T_c in K and β in meV and taking $F_{bs}^* = 2$,

$$T_c\ (\mathrm{K}) = 15.44\,\frac{n_s\beta\ (\mathrm{meV})}{m^{**}/m^*}. \tag{74}$$

Equation (74) accounts for the universal correlation between T_c and $n_s/(m^{**}/m^*)$ observed by Uemura *et al* [34]. From photoemission spectroscopy, we have estimated m^{**}/m^* for Bi-2212 and found it 1.6 for optimally doped samples (appendix A.3). With $n_s = 1$ and $T_c = 80$ K, we obtain from equation (74) 8.29 meV for β. For all cuprates a constant value of β, 8.45 meV for Sr and 10.47 meV for Ba, fits the experimental data on T_C. For metallic Ba and Sr with

Table 2. The calculated values of T_c for oxide superconductors from equation (74). n_{Cu} is the number of copper planes, m^{**}/m^* is the effective mass and n_s is the superconducting carrier density per primitive unit cell. The last column gives the observed values of T_c. n_s is chosen to fit the observed T_c, taking a constant value of β of 10.47 meV for the Ba and 8.45 meV for the Sr compound. For $n_{Cu} = 1$, 2 and 3, m^{**}/m^* is 3.5, 1.6 and 1.3, respectively (see text).

Compound	Short notation	n_{Cu}	m^{**}/m^*	n_s	T_c (K) (cal.)	T_c (K) (obs.)
$La_{2-y}Sr_yCuO_4$ $y = 0.15$	214	1	3.5	1.0	37.3	37
$Bi_2Sr_2CuO_6$	Bi-2201	1	3.5	0.16	6.0	6
$Tl_2Ba_2CuO_6$	Tl-2201	1	3.5	0.32	14.8	15
$HgBa_2CuO_{4+\delta}$	Hg-1201	1	3.5	2.0	92.4	92
$YBa_2Cu_3O_{7-\delta}$	Y-123	2	1.6	0.96	97.0	92
$Bi_2Sr_2CaCu_2O_8$	Bi-2212	2	1.6	1.0	81.5	80
$Tl_2Ba_2CaCu_2O_7$	Tl-2212	2	1.6	0.80	80.8	80
$Tl_2Ba_2CaCu_2O_7$	Tl-2212	2	1.6	1.0	101.0	108
$PbSr_2CaCu_2O_7$	Pb-1212	2	1.6	1.0	81.5	80
$Bi_2Sr_2Ca_2Cu_3O_{10}$	Bi-2223	3	1.3	1.0	100.4	110
$Tl_2Ba_2Ca_2Cu_3O_9$	Tl-2223	3	1.3	1.0	124.3	120
$Tl_2Ba_2CaCu_3O_{10}$	Tl-2213	3	1.3	1.0	124.3	125
$HgBa_2Ca_2Cu_3O_{8-\delta}$	Hg-1223	3	1.3	1.0	124.3	134
$Tl_2Ba_2Ca_3Cu_4O_{11}$	Tl-2234	4	1.35	1.0	119.7	120
$Tl_2Ba_2Ca_3Cu_4O_{12}$	Tl-2234	4	1.5	1.0	107.8	105

$z = 2$ and with the values of Knight shift and nuclear magnetic susceptibility from [27], β from equation (67) is 5.17 meV for Ba and 8.47 meV for Sr, in reasonable agreement with the T_C data.

It is shown by Uemura *et al* [34] that in oxide superconductors the muon-spin-relaxation (μSR) rate, σ, at $T = 0$ K is proportional to the ratio $n_s/(m^{**}/m^*)$. In heavily doped samples, T_C shows saturation and suppression with increasing values of this ratio and saturation starts at different values of σ ($T \to 0$) depending on the multiplicity of CuO planes, n_{Cu}. For example, for n_{Cu}, = 1, the peak in T_C occurs approximately at $\sigma(T \to 0) \sim 1.35\ \mu s^{-1}$, for $n_{Cu} = 2$, at 3.0 μs^{-1}, and for $n_{Cu} = 3.0$, at 3.6 μs^{-1}. If we assume that the peak occurs at optimally doped compositions for which $n_s = 1$, and for $n_{Cu} = 2$, $m^{**}/m^* = 1.6$ as experimentally determined for Bi 2212, we get $m^{**}/m^* = 3.5$ for $n_{Cu} = 1$ and 1.3 for $n_{Cu} = 3$. In table 2 we give the values of T_C obtained from equation (74) using the value of effective mass, m^{**}/m^*, 3.5, 1.6 and 1.3 for $n_{Cu} = 1$, 2 and 3, respectively, and with n_s as a fitting parameter. In most cases, $n_s = 1$. However, for Hg-1201, $n_s = 2$, indicating the possibility of two pairons per unit cell. As the μSR data are not available for $n_{Cu} = 4$, for these we have chosen $n_s = 1$ and obtained m^{**}/m^* from equation (74). The effective mass decreases as the number of copper planes increases from one to three, beyond which it begins to increase.

From table 2 we find that values of n_s that are not unity are multiples of 0.16. As n_s is proportional to the product of the probabilities of the pairon in the e- and h-sections of the Fermi surface, $n_s = 1$ represents equal probability, n_s 0.96 represents approximately 48% and 52% and so on. The reason for multiple values of 0.16 for n_s is not clear at present.

7. Structure dependence of superconductivity and maximum critical temperature

The phonon mediated coupling presented here is in the isotropic and homogeneous model of a metal. From equation (64) T_c is directly related to F^*_{bs} which is a structure dependent

parameter. It is shown that in Nb_3Sn and V_3Si with A15 structure the increase in T_c to 18.5 and 17.2 K from pure Nb and V value of T_c, respectively, can be attributed entirely to F^*_{bs}. T_c in these compounds is, however, limited by the factor $M\theta_D$ in the denominator. In MgB_2 and fullerenes, this is small so T_c is relatively large, but in both these compounds isotropy is partially lost, leading to reduction in F^*_{bs}. Optimizing both these factors may lead to a maximum T_c of 40 to 50 K.

The coupling constant ζ of the exciton-coupled superconductor is nearly twice λ^D while θ_D is about one-tenth of E_F. Since the critical temperature is the product of the two and as T_C of the phonon-coupled superconductor can barely exceed 20 K, with appropriate optimization T_C (exciton) may reach 300 K.

8. Conclusion

It is shown that the pairing correlations that makes the electron–ion repulsive energy from the Darwin term vanish produce electron–electron coupling through recoilless scattering and are of two kinds, one phonon induced and the other exciton induced. The former predominates in low T_c while the latter in high T_c superconductors. For the dominant phonon-coupled system there is near ideal isotope effect and the phonon spectral function obtained from tunnelling is similar to the phonon density of states from neutron scattering as both are based on a delta-function type of interaction. The magnitude of Coulomb pseudopotential is accounted for by the cancellation theorem, which weakens the attractive bare ion potential within the core of the atom. The critical temperature is obtained from the requirement that the recoil energy of the nucleus in the scattering of the pairon equals the Debye–Waller exponent times the average energy of the boson field. The criterion for superconductivity is expressed in terms of non-vanishing structural weight of reciprocal lattice vectors that transform particles of one band to another and produce the order parameter. The present analysis of critical temperature is based on the superfluid state with vanishing momentum. Its extension to non-vanishing momentum will be important from the point of view of technical application.

Acknowledgment

I am grateful to Professor S H Patil for many critical comments and discussions during the preparation of the manuscript.

Appendix. The effective mass

We attempt to deduce semi-empirically the effective mass of the electron due to electron–phonon, electron–lattice and electron–electron interactions. The aim is limited to the problem of superconductivity.

A.1. Electron–phonon interaction

McMillan [6] has shown that the effective mass due to Fröhlich type ep interaction is determined by equation (11)

$$\frac{m^*}{m_c} = Z(0) = 1 + \lambda. \tag{A.1}$$

To analyse the dependence of λ on materials properties McMillan expressed λ in terms of the ionic pseudopotential

$$\lambda = \frac{N(0)\left\langle I^2\right\rangle}{M\left\langle\omega^2\right\rangle} \tag{A.2}$$

where $I = \mathrm{i}(k-k')\epsilon_{k-k',\nu}v_{k-k'}$.

Here $v_{k-k'}$ is the Fourier transform of the ionic pseudopotential. Equation (A.2) is equation (49) with $v_{k-k'}$ describing the inelastic incoherent scattering cross section due to $\boldsymbol{E}\cdot\boldsymbol{p}$ ionic pseudopotential (equation (48)). We can then take m_c to denote the Coulomb and band dressed effective mass. For the s electron, in addition to incoherent, there also exists a coherent $\boldsymbol{E}\cdot\boldsymbol{p}$ scattering that produces the electron–phonon coupling λ^D given in equation (55). Then

$$\frac{m^{**}}{m^*} = 1+\lambda^D$$

so

$$\frac{m^{**}}{m_c} = Z'(0) = (1+\lambda)\,(1+\lambda^D). \tag{A.3}$$

The renormalization $Z'(0)$ appears in the McMillan experimentally adjusted T_c equation [6].

A.2. Electron–electron interaction

The effective mass within the RPA approximation has been calculated by Quinn and Ferrell [35] and is given by

$$\frac{m}{m_c} = 1 - \frac{ar_s}{2\pi}\left[2+\ln\left(\frac{ar_s}{\pi}\right)\right] \tag{A.4}$$

where $a = ((4/9)\pi)^{1/3}$ and r_s is the interelectron separation parameter. But unfortunately the region of metallic densities lies outside the region of the validity of the RPA, namely $r_s < 1$. The calculation of Rice [36] of m_c/m for metallic densities $1.8 \leqslant r_s \leqslant 2.5$ shows that it is nearly equal to unity.

In the present case for the pairon the ee interaction is taken into account through the screening of the pseudopotential in equation (56) that gives $z' = z - 0.25$ for $|\omega| \leqslant \omega_D$ and $z' = -0.25$ for $\omega_D \leqslant \omega \leqslant E_F/\hbar$. The mass enhancement due to electron–electron interaction is therefore included in the expression for T_C in equation (60).

A.3. Electron–lattice interaction

The mass enhancement for the conduction electron due to its interaction with the electron–ion pseudo-potential is given by [14]

$$\frac{m^*}{m} = m_K m_E = 1+\lambda_{el}. \tag{A.5}$$

Here the component m_K arises from the dependence of energy on the wavevector near the zone boundary and m_E arises from the energy dependence of the bandgap. For Pb, $m_K = 0.95$ and $m_E = 0.91$, hence $\lambda_{el} = -0.14$. Physically the band dressing in Pb reduces the mass of the electron.

In ionic crystals the electron carries with it a cloud of phonons when it moves in the solid. This increases the effective mass of the polaron. In the weak coupling approximation [23]

$$m^{**} \cong m^*\,(1-\tfrac{1}{6}\alpha)^{-1} \tag{A.6}$$

where m^* is the Fröhlich type ep enhanced effective mass and α is the dimensionless coupling employed in polaron theory. The charge conduction is often considered in term of large, small and correlated polarons [32]. The large polarons move in a band and the effective mass is given in equation (A.6). The small polarons are localized states trapped near a single ion and conduction is through thermally activated hopping, which arises due to Franck–Condon transitions. In mixed valence compounds like magnetite and oxide superconductors the conduction occurs through correlated polarons where hopping by small polarons is without Franck–Condon transitions, resulting in vanishing activation Energy, and the effective mass is similar to that in a polaron band [37]. Using equation (A.6) we obtain m^{**}/m^* in Bi-2212 superconductor from photoemission spectroscopy and estimate that for optimally doped samples $\alpha \sim 2.25$ which gives $m^{**}/m^* = 1.6$ [32].

References

[1] Schrieffer J R 1964 *Theory of Superconductivity* (New York: Benjamin)
[2] Allen P B and Metrovic B 1982 *Solid State Phys.* **37** 1
[3] Anderson P W 1987 *Science* **235** 1196
Anderson P W *et al* 1998 *Phys. Rev. Lett.* **58** 2790
[4] Carbotte J P *et al* 2000 *Nature* **401** 354
[5] Nagamatsu J *et al* 2001 *Nature* **410** 63
[6] McMillan W L 1968 *Phys. Rev.* **167** 331
[7] Srivastava C M 1984 *Bull. Mater. Sci.* **6** 273
Srivastava C M 1985 *Pramana J. Phys.* **25** 617
Srivastava C M 1987 *Pramana J. Phys.* **29** L423
[8] Essen H 2000 *Preprint* cond-mat/0002096
Essen H 1999 *J. Phys. A: Math. Gen.* **32** 2297
[9] Hirsch J E 2005 *Preprint* cond-mat/0508471
Hirsch J E 2005 *Phys. Rev.* B **71** 184521
[10] Mattheiss L F and Hamann D R 1983 *Phys. Rev.* B **28** 4227
[11] Bachelet G B and Schuter M 1982 *Phys. Rev.* B **25** 2103
[12] Scalapino D J 1964 *Superconductivity* vol 1, ed R D Parks (New York: Dekker) p 449
[13] Lipkin J 1961 *Phys. Rev.* **123** 62
[14] Cohen M L and Heine V 1970 The fitting of psuedopotentials to experimental data *Solid State Phys.* **24** 37
Heine V and Weaire D 1970 Pseudopotential theory of cohesion and structure *Solid State Phys.* **24** 249
[15] See chapter 1 in Ginzburg V L and Kirzhnits D A (ed) 1982 *High Temperature Superconductivity* (New York: Consultant Bureau) p 23 for exciton and chapter 3, p 126 for electron–ion interaction (English translation by A K Agyeil and J L Birman)
[16] Springford M (ed) 1980 *Electrons at the Fermi Surface* (Cambridge: Cambridge University Press) p 70
[17] Hopfield J J 1989 *Phys. Rev.* B **86** 443
[18] Bethe H A and Salpeter E E 1957 *Handbuck der Physik* vol 35/1, ed S Flugg (Berlin: Springer) p 159
[19] Ambegaoker V 1964 *Superconductivity* vol 1, ed R D Parks (New York: Dekker) p 259
[20] Ginzburg V L and Landau L D 1950 *Zh. Eskp. Theor. Fiz.* **20** 1064
[21] Glauber R J 1955 *Phys. Rev.* **98** 1962
[22] Placzek G and van Hove L 1954 *Phys. Rev.* **93** 1207
[23] Kittel C 1966 *Quantum Theory of Solid* 3rd edn (New York: Wiley) p 140 for polaron and p 390 for recoilless emission
[24] Oskataki V S 1967 *Sov. Phys.—Solid State* **9** 420
Bredov M M *et al* 1967 *Sov. Phys.—Solid State* **9** 214
[25] Morel P and Anderson P W 1962 *Phys. Rev.* **125** 1263
[26] Visscher W M 1960 *Ann. Phys.* **9** 194
[27] Carter G C, Bennett L H and Kahan D J 1977 *Progress in Materials Science* vol 20 *Metallic Shifts in NMR* Part I (New York: Pergamon)
[28] Anderson J K and Gold A V 1965 *Phys. Rev.* **139** A1459
[29] Cracknell A P and Wong K C 1973 *The Fermi Surface* (Oxford: Clarendon)
[30] Louie S G and Cohen M L 1974 *Phys. Rev.* B **10** 3237

[31] Mattheiss L F 1975 *Phys. Rev.* **12** 2161
[32] Srivastava C M 1998 *Pramana J. Phys.* **50** 11
[33] Mazim I I *et al* 1992 *Phys. Rev.* B **45** 5103
[34] Uemura Y J *et al* 1989 *Phys. Rev. Lett.* **62** 2317
[35] Quinn J J and Ferrell R A 1958 *Phys. Rev.* **112** 812
[36] Rice T M 1965 *Ann. Phys.* **31** 100
[37] Srivastava C M 1991 *Physica* C **176** 481